Electronics, Communications and Networks
A.J. Tallón-Ballesteros et al. (Eds.)

doi:10.3233/FAIA231256

Low Overhead Adaptive Channel Equalizations for Upstream Burst Reception in 200Gbps Intensity Modulation-Coherent PONs

Yuanzhe SUN[1], Tao YANG[1,*], Xue CHEN[1], Yi XIAO[1], Xingang HUANG[2], Zhuang MA[2], Yiming ZHONG[2] and Bo LIU[2]

[1] *State Key Laboratory of Information Photonics and Optical Communications, Beijing University of Posts and Telecommunications, Beijing 100876, China*

[2]*ZTE Corporation, Shanghai, 201203, China*

Abstract. This paper presents a 200Gbps PON uplink burst coherent reception system that utilizes polarization-independent 4PAM optical intensity modulation-polarization diversity. To accommodate the burst changes in the PON uplink, we propose an adaptive channel equalization algorithm based on training sequences. This algorithm is characterized by low overhead, allowing for fast convergence. Simulation results demonstrate that adaptive compensation of PMD is feasible with a mere 18.5ns of preamble overhead. Additionally, by including only one SOA as a pre-amplifier in the OLT, a system power budget exceeding 35dB can be achieved.

Keywords. Intensity modulation, burst coherent reception, adaptive channel equalization

1. Introduction

With the continuous development of emerging network technologies and the emergence of high-bandwidth services, Internet traffic has shown explosive growth, and users' demand for network bandwidth has been increasing. Passive optical networks, due to their relatively low cost and smooth upgrades, have become the most commonly used optical access method for operators [1]. At the same time, PON have the potential for various applications [2-3]. In recent decades, TDM-PON has emerged as a popular solution for access networks due to its wavelength resource efficiency, mature technology, simple structure, and low cost [4]. Existing research demonstrates the feasibility of high-bandwidth devices in TDM-PON. However, to account for the cost sensitivity of access networks, the current mainstream trend is towards high-speed PON based on low-bandwidth devices. Meanwhile, the realization of larger branching ratios and multi-user requirements necessitates high power budgets. The optical link power budget is dependent on incident optical power and receiver sensitivity. Therefore, the use of coherent detection technology with high sensitivity is gradually emerging as a

[1]Corresponding author: Tao Yang, Beijing University of Posts and Telecommunications, Beijing 100876, China; E-mail: yangtao@bupt.edu.cn.

promising solution for high-speed PON. The advantage of coherent detection technology is its ability to enhance receiver sensitivity through the local oscillation laser, thereby meeting the requirements of the power budget. However, the higher demands placed on modulators and receivers, coupled with the technical challenge of resolving the critical task of low-latency, low-overhead burst coherent reception DSP processing, present significant obstacles.

The high-speed PON uplink typically employs the IMDD scheme. Optimizations for this scheme commonly focus on two areas: improving DSP algorithms and expanding ONU capacity through branching ratio or power budget enhancements. Examples of such optimizations include the OFDMA direct detection scheme, which reduces DSP complexity [5], and the 50Gbps equalization-free IMDD scheme [6]. Although system performance improves to a certain extent after optimization, it remains inadequate in achieving high power budget at a low cost, and presents technical challenges such as high system cost and algorithm complexity. Furthermore, polarization mode dispersion (PMD) plays a crucial role in limiting the enhancement of system performance. For the 200Gbps coherent PON system, burst mode is utilized in the uplink via time division multiplexing access for transmitting data from ONU to OLT. It should also be noted that multiple ONUs correspond to one OLT, making it crucial to address the task of minimizing the cost of sending ONUs' terminals. At the same time, it is necessary to address the issues of high overhead, varying damages to packets in burst mode, and time-varying system characteristics. To mitigate the impact of dynamically changing polarization mode dispersion (PMD), a low overhead adaptive channel equalization algorithm must be developed.

To accomplish the high power budget target of a PON system at a low cost, this paper presents a 200Gbps PON uplink 4PAM intensity modulation-polarization diversity burst coherent reception scheme, addressing the technical complexities involved. Additionally, we propose and demonstrate an adaptive channel equalization algorithm based on training sequences for dynamically changing PMD. The suggested adaptive channel equalization algorithm can achieve fast convergence and result in significantly low overhead. Simulation results demonstrate that adaptive compensation for dynamically changing PMD is achievable with a mere 18.5ns of preamble overhead. Further, introducing a single SOA as a pre-amplifier in OLT can actualize the system power budget of over 35dB.

2. Principle

2.1. 200Gbps PON uplink 4PAM intensity modulation polarization diversity coherent reception overall scheme

The cost of the entire uplink system is mainly concentrated on the ONU side. By utilizing the easy-to-integrate EA optical intensity modulation in the 200G PON uplink, it reduces the demand for ONU carrier lasers and local oscillation lasers. The transmitter side can apply Nyquist shaped filtering to lower bandwidth requirements. Furthermore, the OLT receiver terminal implements coherent reception with improved sensitivity for achieving the high power budget. To overcome the impact of random polarization rotation, polarization sensitivity in coherent detection, and achieve coherent reception independent of polarization, implementing polarization diversity reception at the receiving terminal is necessary. The implementation of balanced coherent reception, utilizing a 90-degree mixer, reduces performance demands on transceiver lasers and mitigates frequency offset and linewidth influence on the receiving terminal's system performance. To achieve a high power budget target at a low cost, the uplink scheme [8-9] used in this study for the 200G PON system employs 4PAM optical intensity modulation, utilizing an EA modulator at ONU. Additionally, burst coherent reception is achieved at the OLT through SOA pre-amplifier [10].

The established uplink system for coherent reception of bursts, employing polarization diversity and intensity modulation with Nyquist-PAM4, is visually depicted in Figure 1.

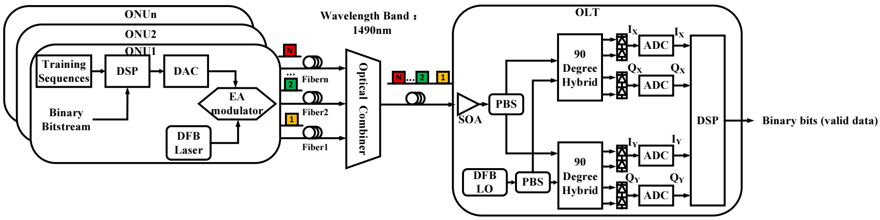

Figure 1. PAM4 intensity modulation polarization diversity coherent burst reception in PON uplink

The transmitter DSP is depicted in Figure 2.

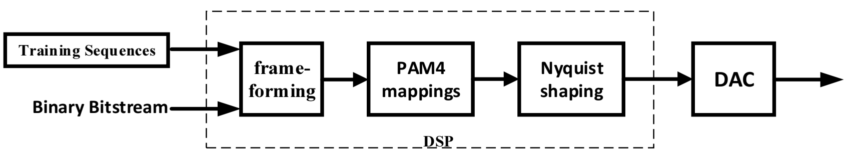

Figure 2. ONU transmitter DSP

The data frame structure for burst packets in the TDM-PON data assistance arrangement is shown in Figure 3. SP1 functions as a protection header to prevent truncation of the synchronization header SP2. The synchronization symbol SP2 can choose two identical randomly generated sequences due to the efficient self-correlation property of the pseudo-random sequence. The first half of the symbols are randomly generated, while the second half is the same as the first. SP3 is used for PMD equalization and consists of a readily available piece of randomly generated data.

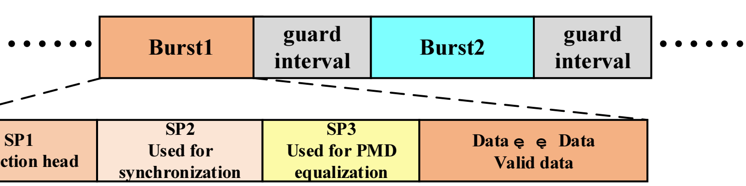

Figure 3. Burst Packet Data Frame Structure

For the 200Gbps PON uplink, CD and PMD are the primary causes of optical signal damage during transmission when using a polarization independent 4PAM intensity-only polarization diversity burst coherent receiver system. Additionally, the TDM-PON transmits information data from various ONUs through different time slots, making burst time-slot synchronization essential for effectively equalizing and processing the transmission signals. Given the reliability, stability, and fast convergence characteristics of the data-assisted DSP scheme, the overall DSP processing scheme employs the data-assisted approach utilizing training sequences. Dispersion compensation, an unsupervised algorithm, is accomplished prior to burst time-slot synchronization. The receiver's DSP utilizes the Overlap Frequency Domain Equalization (OFDE) method for dispersion compensation. For achieving burst time-slot synchronization, the SP2 employs the Schmidl synchronization algorithm, which precisely locates the preamble code. Once the exact location of the preamble code, SP3, is determined by utilizing the burst time slot synchronization algorithm, we proceed with executing data-assisted LMS-based PMD equalization utilizing the SP3 training sequence. The block diagram of the DSP on the receiver side is presented in Figure 4.

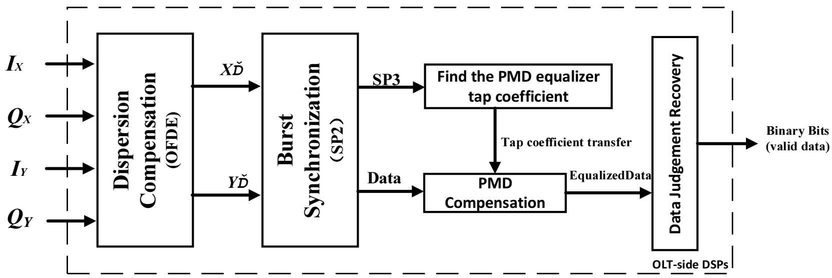

Figure 4. OLT receiver DSP block diagram

2.2. Adaptive channel equalizations

The data-assisted PMD equalization method largely utilizes Finite Impulse Response (FIR) filters for PMD compensation. This involves obtaining PMD equalizer tap coefficients via training sequences and then using multi-tap FIR filters with different tap weights to achieve effective data PMD compensation.

The LMS-based equalization method, assisted by data, initially identifies the locations of the training sequence SP3 through a burst time slot synchronization algorithm. The error function ε for the gradient descent algorithm is obtained by utilizing the fact that the original SP3 transmitted is already known.

Initialize the FIR filter by setting each tap with the center tap coefficient of the filter as 1 and the non-center tap coefficients as 0. Use X to refer to the impaired received training sequence and D for the sent known training sequence:

$$h_{Equa,0} = [0,0,\cdots 1,\cdots,0,0] \tag{1}$$

The training sequence X, with x being a dimension of N x 1, is fed sequentially into the equalization filter. Each input represents a range of data, from the 1st to the Nth data for the first input, the 2nd to the N+1th data for the second input, and so on. The resulting output of the filter, Y, can be expressed as follows.

$$Y = h_{Equa} \cdot x \tag{2}$$

Where h_{Equa} is a 1xN matrix and x is an Nx1 matrix, the resulting Y represents the filter output with dimensions of 1x1. This form of equalization is achieved through matrix multiplication as dictated by the structure of the FIR filter, depicted in Figure 5.

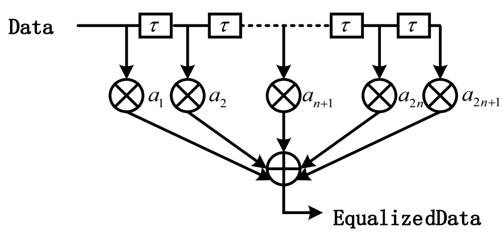

Figure 5. PMD equalizer

The filter equalization process can be equated to matrix multiplication. Subsequently, the error is calculated.

$$\varepsilon = d - Y \tag{3}$$

Where d is the reference signal (ideal signal) acquired from the known training sequence D. The ultimate objective is to accomplish the convergence of the filter equalized output Y to the reference signal d.

The stochastic gradient algorithm yields an update equation for the coefficients of the filter's tap weights.

$$h_{Equa}' = h_{Equa} + \mu\varepsilon Y \cdot x^T \tag{4}$$

The gradient change quantity in Equation (4) is equal to $\varepsilon Y \cdot x^T$, which has dimensions of 1×N, the same as the tap coefficients. The transpose matrix of x, which also has dimensions of 1×N, is represented by x^T in Equation (4). The step for updating the tap coefficients is denoted by u. Substituting the error obtained from Equation (3) into Equation (4), the error is used for updating multiple taps, and the corresponding error is added to each tap through Equation (4) to enable one update of multiple taps. Continuously loop through Equations (2), (3), and (4) until convergence to obtain the coefficients for the filter taps.

The filter tap coefficients can be obtained through the above steps. After acquiring the tap coefficients, the PMD equalizer can be utilized to equalize the valid data. Fig. 5 illustrates the structure of the PMD equalizer with T/2 fractional intervals, where τ represents Ts/2.

3. Simulation

3.1. Simulation platform and simulation parameters

Referring to Fig. 1, the two to one simulation model was built using VPI9.9. The simulation parameters are set as shown in Table 1, with a single polarization state PAM4 signal line rate of 200 Gbps and a line symbol rate of 100 GBaud. The system operates within the S-band wavelength, frequently employed in PON systems. Parameters such as the dispersion and PMD coefficients rely on common values in practical uses.

Table 1. System key parameters

parameter name	**parameter values**	**parameter name**	**parameter values**
ONU transmitter			
Center frequency of ONU1 laser（Hz）	201.34T+1G	Center frequency of ONU2 laser（Hz）	201.34T+15G
Laser linewidth (Hz)	1M(ONU1)/10M(ONU2)	Emission optical power (dBm)	0
transmission link			
Transmission Fiber Lengths（km）	5(ONU1)/20(ONU2)	PMD coefficient($ps/\sqrt{km}$)	0.1
CD coefficient（ps/nm/km）	20	fiber optical attenuation（dB/m）	0.2e-3
OLT receiver			
Local Oscillation laser frequency（Hz）	201.34T	Linewidth of Local Oscillation Laser（Hz）	1M
optical power of local oscillation（dBm）	15	Low-pass filter bandwidth at receiver（Hz）	0.55*Symbol rate
ADC Sampling Rate	2* Symbol rate	Shot noise	ON
PIN Responsivity（A/W）	0.8	Thermal noise power spectral density (A/HZ^(1/2))	1.2e-11
SOA injection current (A)	0.15	Noisefigure corresponding to SOA (dB)	7.5
SOA Gain(dB)	26	noise power spectral density（W/HZ）	1.29e-17

The AmpSOA model in the VPI simulation software is utilized as the SOA model in the simulation, with the ASE noise power spectral density and the noise bandwidth being the main parameters of this module. However, due to coherent reception with wavelength selectivity in the uplink, the noise beyond the signal bandwidth barely impacts the system's performance. It is necessary to consider solely one parameter, the ASE noise power spectral density, which can be calculated using the subsequent equation:

$$Power\ density\ ASE = 0.5 * h * CenterFrequency\ (NoiseFigure * Gain - 1) \tag{5}$$

Where Planck's constant h=6.62607015×10^{-34} J-s, SOA Gain is 26dB, SOA noisefigure is selected according to the actual typical value, and the actual typical value is 7.5dB, and the final calculated ASE noise power spectral density is 1.29*10^{-17} W/HZ.

3.2. Burst synchronization simulation

To quantify the anti-noise performance of synchronization, the reference paper [7] defines the Peak-to-Maximum Noise Ratio (PMNR) as an indicator of the synchronization algorithm's anti-noise performance. A larger PMNR indicates a wider gap between the peak value of the synchronization metering curve and the maximum noise value, resulting in better anti-noise synchronization.

The relationship between PMNR and SP2 synchronization symbol length was simulated and illustrated in Figure 6. The analysis indicates that an increase in SP2 symbols leads to a gradual increase in PMNR. Additionally, a higher PMNR implies that the maximum noise value and peak value gap of the synchronization measurement curve also increases, thereby gradually enhancing the noise immunity of the synchronization.

Too few synchronization symbols are prone to pseudo-synchronization, but under the premise of ensuring the performance, the fewer the synchronization symbols, the better, which is conducive to reducing the overhead, refer to Figure 6, in order to consider the anti-noise performance, set $\frac{\text{peak value}}{\text{maximum noise}} = 2$, which is converted into dB of 3dB, so should be selected when the PMNR $\geq$ 3dB corresponds to the length of the SP2 symbols, SP2 = 400 can meet the requirements. Therefore, the SP2 length of 400 is selected.

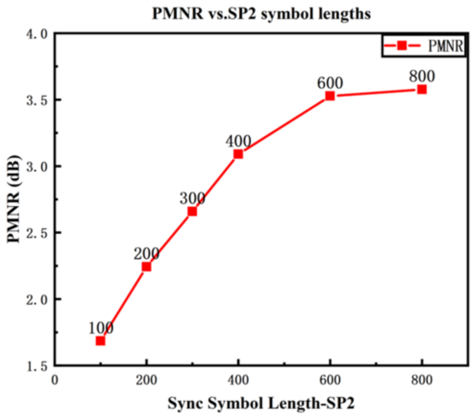

Figure 6. PMNR vs. SP2 symbol lengths

Under the condition that SP2 length is 400, Figures 7 and 8 show the corresponding synchronization measurement curves of the burst packet sent by ONU1 and ONU2 near the receiver sensitivity. It is evident that both figures exhibit significant synchronization peaks, indicating the effective operation of the burst synchronization algorithm.

After applying the burst synchronization algorithm to determine the synchronization heads of burst1 and burst2, it is possible to identify the corresponding SP3 positions and valid data positions of burst1 and burst2. The LMS can then equalize the PMD based on the training sequence.

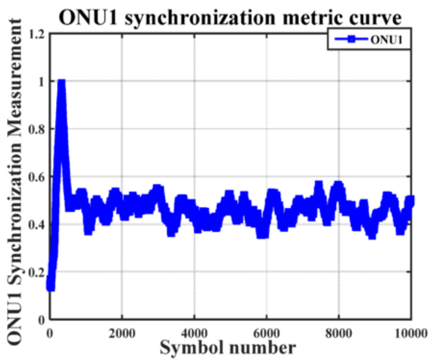

Figure 7. ONU1 synchronization metric curve

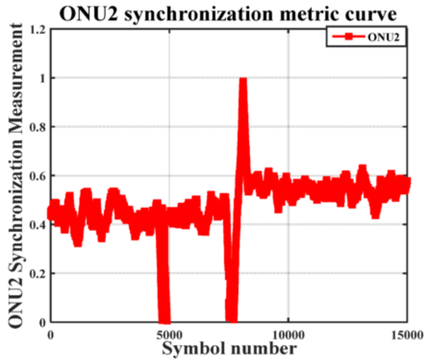

Figure 8. ONU2 synchronization metric curve

3.3. Adaptive channel equalizations simulation

According to the convergence of MSE in the actual simulation, the MSE criterion is set to 0.06, and the burst packet sent by ONU1 is transmitted in Nyquist point-to-point 5km transmission, with laser frequency offset of 1GHZ, laser linewidth of 1MHz at the transmitter terminal, and low-pass filter bandwidth of 55GHZ at the receiver terminal, and the MSE vs. symbols is obtained from the simulation near the sensitivity of the receiver as shown in Fig. 9, which shows that the MSE curve begins to converge at the 200th symbol. Thus, under the condition of 5km transmission, SP3 corresponds to 200 symbols.

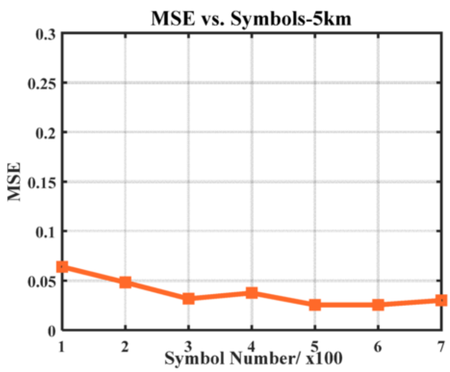

Figure 9. MSE vs. symbols-5km

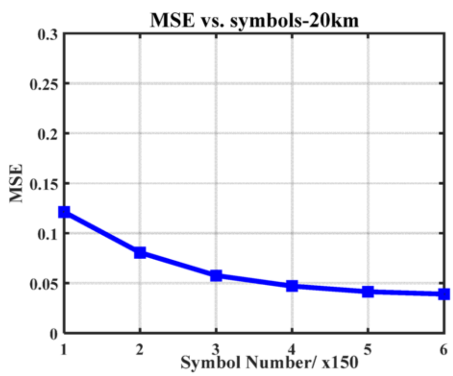

Figure 10. MSE vs. symbols-20km

The MSE criterion remains at 0.06. ONU2's burst packet is transmitted via Nyquist point-to-point 20km transmission, with a laser frequency offset of 15GHz, transmitter laser linewidth of 10MHz, and receiver low-pass filter bandwidth of 55GHz. The MSE vs. symbol number curve, obtained via simulation near receiver sensitivity, is shown in Fig. 10 and converges after the 450th symbol. Therefore, under the condition of 20km transmission, the number of symbols for SP3 is 450.

In summary, for a fiber transmission length of 5 km (ONU1), there are 200 symbols corresponding to SP3. For a fiber transmission length of 20 km (ONU2), there are 450 symbols corresponding to SP3. The total length of the training sequence is 800 for ONU1 and 1050 for ONU2. Consequently, achieving the PMD adaptive compensation only requires 18.5ns of preamble overhead.

3.4. System simulation

The curve depicting the variation of overall average BER with the receiver's optical power acquired from the simulation is exhibited in Figure 11.

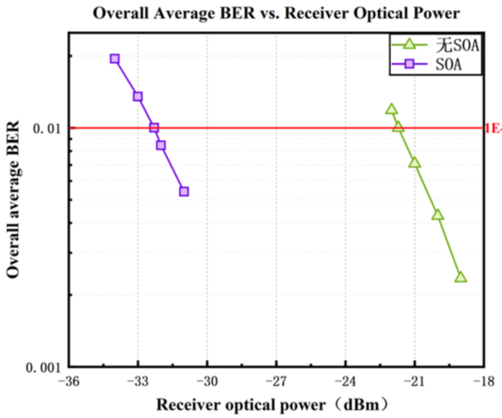

Figure 11.Overall Average BER vs. Receiver Optical Power

As illustrated in Figure 11, the receiver sensitivity of the two-to-one burst coherent receiver system is -21.71 dBm without SOA, but with SOA added, the receiver sensitivity improves by 10.59 dB to -32.3 dBm.

Under the given conditions, where the transmit optical power of two ONUs is at 3 dBm, the simulation shows that the receiver sensitivity is -32.3 dBm, and the power budget of the system is 35.3 dB. Therefore, to exceed the power budget of 35 dB, the transmit optical power of the ONUs must be greater than 3 dBm. After simulating, it has been verified that fiber nonlinear effects are stimulated when the incoming optical power is 15 dBm or above. However, if the ONU transmit optical power meets the conditions of 3dBm⩽ONU transmit optical power < 15dBm, then not only will the optical fiber nonlinear effect not be stimulated, but it will also achieve a super 35 dB power budget.

4. Conclusions

This paper presents a coherent reception scheme for the 200Gbps PON uplink utilizing 4PAM intensity modulation and polarization diversity burst. In addition, an adaptive channel equalization algorithm, which is demonstrated through training sequences, addresses dynamically changing PMD. Due to the algorithm's low overhead, swift convergence is facilitated. Simulation results demonstrate the feasibility of adaptively compensating for dynamically changing PMD by using only 18.5ns of preamble overhead. Implementing a single SOA as a pre-amplifier in the OLT achieves a system power budget of over 35dB.

Funding. This work was supported by ZTE Industry-University-Institute Cooperation Funds (No. HC-CN-20230105001), Fundamental Research Funds for the Central Universities(2023PY08), Fundamental Research Funds for the Central Universities (No. 2022RC09), State Key Laboratory of Information Photonics and Optical

Communications (No. IPOC2021ZT17), National Natural Science Foundation of China (No. 62001045).

References

[1] Luo Siyu, Xu Yan, Li Zhengxuan, et al. "Research progress on key physical layer technologies in next-generation optical access networks ," Journal of Applied Science, 2020,38 (04): 612-629.

[2] Sharma, Vishal, and Subhashish Banerjee. "Analysis of quantum key distribution-based satellite communication." In 2018 9th International Conference on Computing, Communication and Networking Technologies (ICCCNT), pp. 1-5. IEEE, 2018.

[3] Sharma, Vishal, and Asha Bhardwaj. "Analysis of Differential Phase Shift Quantum KeyDistribution using single-photon detectors." In 2022 International Conference on Numerical Simulation of Optoelectronic Devices (NUSOD), pp. 17-18. IEEE, 2022.

[4] Li Jie,"Research on Future Oriented Coherent PON Systems and Key Algorithms for Coherent DSP ," Huazhong University of Science and Technology, 2021.

[5] B. Lian, N. Feng and Z. Wei, "A Novel Scheme to Reduce the ONU's DSP Complexity for IMDD-OFDMA-PON," 2022 20th International Conference on Optical Communications and Networks (ICOCN), Shenzhen, China, 2022, pp. 1-3.

[6] R. Borkowski, H. Schmuck, G. Cerulo, H. Debrégeas and R. Bonk, "Single-Wavelength Symmetric 50 Gbit/s Equalization-Free NRZ IM/DD PON with up to 33 dB Loss Budget and Fiber Transmission over >40 km," 2019 Optical Fiber Communications Conference and Exhibition (OFC), San Diego, CA, USA, 2019, pp. 1-3.

[7] J. Zhang, Z. Jia, M. Xu, H. Zhang and L. Alberto Campos, "Efficient preamble design and digital signal processing in upstream burst-mode detection of 100G TDM coherent-PON," in Journal of Optical Communications and Networking, vol. 13, no. 2, pp. A135-A143, February 2021.

[8] R. Koma et al., "Demonstration of Real-Time Burst-Mode Digital Coherent Reception With Wide Dynamic Range in DSP-Based PON Upstream," in Journal of Lightwave Technology, vol. 35, no. 8, pp. 1392-1398, 15 April15, 2017.

[9] R. Koma, M. Fujiwara, J. Kani, K. Suzuki and A. Otaka, "Burst-mode digital signal processing that pre-calculates FIR filter coefficients for digital coherent pon upstream," in Journal of Optical Communications and Networking, vol. 10, no. 5, pp. 461-470, May 2018.

[10] J. Zhang et al., "SOA Pre-Amplified 100 Gb/s/λ PAM-4 TDM-PON Downstream Transmission Using 10 Gbps O-Band Transmitters," in Journal of Lightwave Technology, vol. 38, no. 2, pp. 185-193, 15 Jan.15, 2020.